International Journal of Engineering Research & Technology (IJERT)
ISSN: 2278-0181
Vol. 4 Issue 11, November-2015

Controller Design for Line of Sight Stabilization System

A. G. Habashi, M. M. Ashry, M. H. Mabrouk,
and G. A. Elnashar.
MTC, Cairo, Egypt

***Abstract*—For any fire control system, performance improvement of Line Of Sight (LOS) stabilization subsystem enhances its mission capabilities. Designing controllers for a LOS stabilization subsystem, which is subjected to model uncertainty, is an interesting and challenging problem. In this paper different control techniques for LOS stabilization subsystem are used. The designed controllers are classical Proportional-Integral (PI) controller, genetically tuned PI controller, Linear Quadratic Regulator (LQR) controller, Linear Quadratic Gaussian (LQG) controller, and H_∞ controller. Their performances in normal conditions are compared. They are also compared from robustness to model uncertainty point of view. Simulation results are used to determine the effectiveness of each controller in normal conditions and also when the system is subjected to model uncertainty.**

Keywords*—Classical Proportional-Integral (PI) Controller; Genetically Tuned PI controller; Linear Quadratic Regulator (LQR) Controller; Linear Quadratic Gaussian (LQG) Controller; H_∞ Controller.

I. INTRODUCTION

Stabilized platform has many uses in various applications. One of the most common applications is in stabilization of the Line Of Sight (LOS) systems. Sensing equipments such as, electronic imaging devices, cameras, radars, and navigation instruments are operated in moving vehicles that may be undertake rotational motion around their center of rotations. In such an environment, because of the disturbance from the carrier, these equipments cannot work normally and finally lose their functions. In order to guarantee accurate performance, (LOS) stabilization technology is used to isolate LOS sensors from carrier disturbance. The LOS stabilization system is a system that keeps the sightline of an electro-object sensor when it is exposed to external disturbance such as base motion[1].

The main function of LOS stabilization systems can be defined briefly as maintaining or controlling the LOS of one object relative to another one. To achieve this function many control techniques have been proposed. A composite scheme, use a Proportional-integral-derivative (PID) and adaptive control to control a gyro mirror of LOS system, is proposed by K.K. Tan et al [2]. The effectiveness and applicability of the proposed control scheme are verified by Simulation and real-time experimental. Another control scheme was proposed a proportional-integral-double integral (PII2) controller for gyro stabilization electro-optical platform [3]. In this platform the most important index that must be put forward is the zero steady state error index. Analysis were firstly done on two classical control schemes, the first scheme based on angle feedback using gyro designed in frequency domain. The second scheme introduced was the rate gyro feedback scheme using PID compensator [4]. A stabilized platform has been introduced with double closed loop control system. Speed feedback loop is designed using PID controller and displacement feedback loop is designed using Fuzzy Neural Network (FNN) controller. A development of the angular rate kinematics equations is represented for the non-linear coupled mirror LOS stabilization system [5]. Another system for stabilizing platform of a ship carried antenna and its core component, is discussed to develop a control system composed of three control loops, each of which is associated with a single-variable controller [6]. First, PID controller was applied; then, Takagi-Sugeno fuzzy controller was used for controlling the platform. Simulation tests were established and the results have demonstrated the effectiveness of the proposed Takagi-Sugeno fuzzy controller comparing to the PID controller.

PID controllers are commonly used in industrial controlled systems as a result of the reduced number of tuned parameters [7]. Under the linear conditions of the process, classic PID controller can reach the required performance. But, under the conditions with nonlinear constraints and uncertainties the classical PID controller is hard to achieve the system desired performance with the required accuracy [8]. The uncertainties in the model may come from un-modeled dynamics, parameter variations, linearization of nonlinear elements, etc. The controller that guarantee stability and provide satisfactory performance in the presence of model uncertainties, is called robust controller [9].

In this paper, different control techniques for controlling LOS system will be designed and compared to select the best technique that achieve acceptable system performance and to be robust to model uncertainty.

II. SYSTEM DESCRIPTION

The system under investigation is a dual axes stabilized platform that consists of inner and outer gimbals, each of position is determined by the elevation angle θ_1 and the azimuth angle θ_2 respectively. Two armature current controlled DC motor is used to drive each rotating axis. The inertial angular velocities in both elevation and azimuth directions are measured using two optical fiber gyros. In addition, two optical encoders are used to measure the angular position of each axis. These gyros and encoders are used for feedback control of the system.

Figure (1) shows the 3D solid modeling that is designed on pro/E software for calculation of the system parameters [10]. Figure (2) illustrates the block diagram of the system.

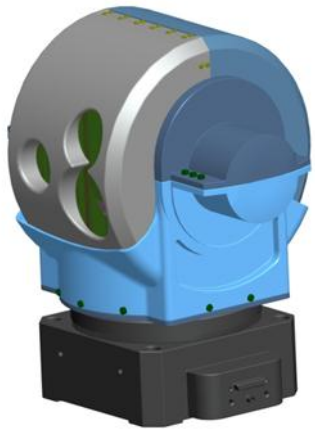

Fig.(1): 3D solid modeling of the dual axis stabilized platform [10].

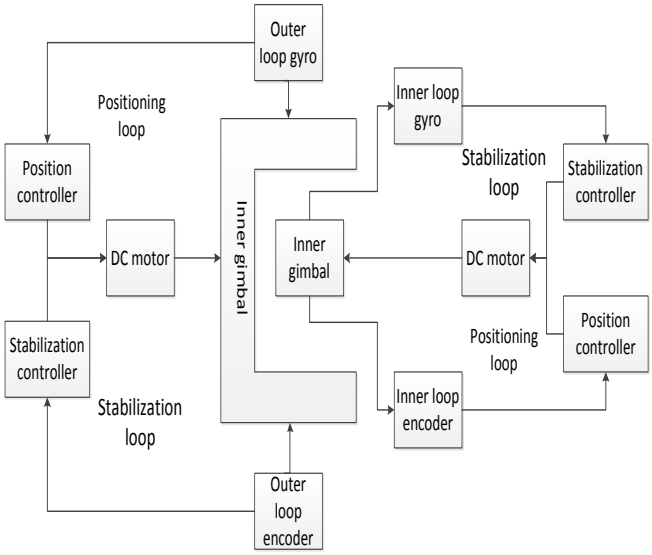

Fig.(2): The power train flow chart of the system.

By defining the Euler angles, transformation matrices and dynamic equations of the system, the dual axis inertial stabilized platform can be represented through the following two second order differential equations given in (1) and (2)

$$\frac{d^2\theta_1}{dt^2} = -\left(\frac{K_m K_b + K_{If} R_a}{R_a I_{Iy}}\right)\frac{d\theta_1}{dt} + \frac{K_m}{R_a I_{Iy}} v_a(t) \qquad (1)$$

$$\frac{d^2\theta_2}{dt^2} = -\left(\frac{K_m K_b + K_{Of} R_a}{R_a I_{Oz}}\right)\frac{d\theta_2}{dt} + \frac{K_m}{R_a I_{Oz}} v_a(t) \qquad (2)$$

where:

$v_a(t)$ Armature volt.
K_m Motor torque constant.
K_b Back electromotive-force voltage constant.
K_f Field winding constant.
K_{If} Field winding constant for inner gimbal motor.
K_{Of} Field winding constant for outer gimbal motor.
R_a Armature winding resistance (ohms).
I_{Iy} mass moment of inertia around y axis for inner gimbal.
I_{Oz} mass moment of inertia around z axis for outer gimbal.

The transfer function of a linear, time-invariant, differential equation system is calculated as in [11]. By taking the Laplace transform for both differential equations given in (1) and (2), equation (3) and equation (4) can be obtained:

$$\theta_1(s)s^2 = -\frac{K_m K_b}{R_a I_{Iy}}\theta_1(s)s - \frac{K_{If}}{I_{Iy}}\theta_1(s)s + \frac{K_m}{R_a I_{Iy}}V(s) \qquad (3)$$

$$\theta_2(s)s^2 = -\frac{K_m K_b}{R_a I_{Oz}}\theta_2(s)s - \frac{K_{Of}}{I_{Oz}}\theta_2(s)s + \frac{K_m}{R_a I_{Oz}}V(s) \qquad (4)$$

Rearranging equation (3) and equation (4), the transfer functions of the inner and outer gimbals models as a relation between input voltage and output angular position can be written as in equation (5) and equation (6):

$$G_{el}(s) = \frac{\theta_1(s)}{V(s)} = \frac{\frac{K_m K_b}{R_a I_{Iy}}}{s\left(s + \frac{K_m K_b + K_{If} R_a}{R_a I_{Iy}}\right)} \qquad (5)$$

$$G_{az}(s) = \frac{\theta_2(s)}{V(s)} = \frac{\frac{K_m K_b}{R_a I_{Oz}}}{s\left(s + \frac{K_m K_b + K_{Of} R_a}{R_a I_{Oz}}\right)} \qquad (6)$$

The physical parameters of gimbals, actuators, and sensors that used in simulation are listed in table (1).

Table (1): The physical parameters of the system.

		Inner gimbal	Outer gimbal
Moment of inertia		0.0289536 Kg.m^2	0.01150 Kg.m^2
Motor parameter	Type	S-50-39-A	S-50-39-A
	R_a	6.6 (ohms)	6.6 (ohms)
	L_a	1.5 (mH)	1.5 (mH)
	K_b	0.098 v/rad/s	0.098 v/rad/s
	K_m	0.12	0.12
Gyro	Type	ARS-15 MHD	ARS-15 MHD
	Scale Factor	1v/(rad/s)	1v/(rad/s)

III. CONTROLLERS

The controller should be able to compensate for disturbance signals. Although faster angular rate response will result in smaller steady state angle tracking errors and faster disturbance rejection capabilities, a response that too fast will lead to instability.

With the above consideration, the following specifications are set for both azimuth and elevation controllers:

- Settling time less than 0.25s.
- Overshoot of less than 20%.
- Zero steady state error.

A. *Design of PI Controller*

Based on the minimization of integral of time weighted absolute error index [12], a PI controller with pre-filter is designed as in figure (3). Dynamic performance is discussed for settling time, overshoot and steady state error.

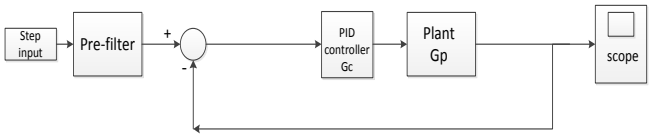

Fig.(3): Block diagram of the plant model under a PI controller.

The optimal PI controller parameters are K_P=63.6, K_I=1300. To improve the overshoot and eliminate the zeros in the closed-loop system transfer function, a pre-filter $G_F(s)$ is designed as:

$$G_F = \frac{1300}{63.6\,S + 1300} \qquad (7)$$

The system response with the pre-filter to a unit step input is shown in figure (4). From this figure; the settling time T_S=0.241s, the percentage overshoot P.O=4.6%, and a zero steady state error is achieved. These results obtained satisfy all the required performance parameters discussed.

B. *Genatically tuned PI Controller*

Genetic Algorithm (GA) is a stochastic algorithm depending on principles of genetics and natural selection. Genetic Algorithms (GAs) are a stochastic global search method that simulates the process of regular evolution [13]. The tuning of the PI controller parameters (K_P, K_I) by using GA will achieve the optimal values for these parameters based on minimizing the Mean Square Error (MSE) of the controlled system.

The block diagram for the controlled system is given in figure (5).

The genetic algorithm parameters chosen for the tuning purpose are shown in table (2).

The resulting controller parameters chosen using GA are K_P= 652.167, K_I= 60.794. these results produced after 58 iteration process by using GA toolbox in Matlab [14].

Figure (6) shows the resulting output response of the system by using values of Genetically tuned PI controller parameters. From this figure; the settling time T_S=0.0966, percentage overshoot P.O=0.077%, and a zero steady state error is achieved.

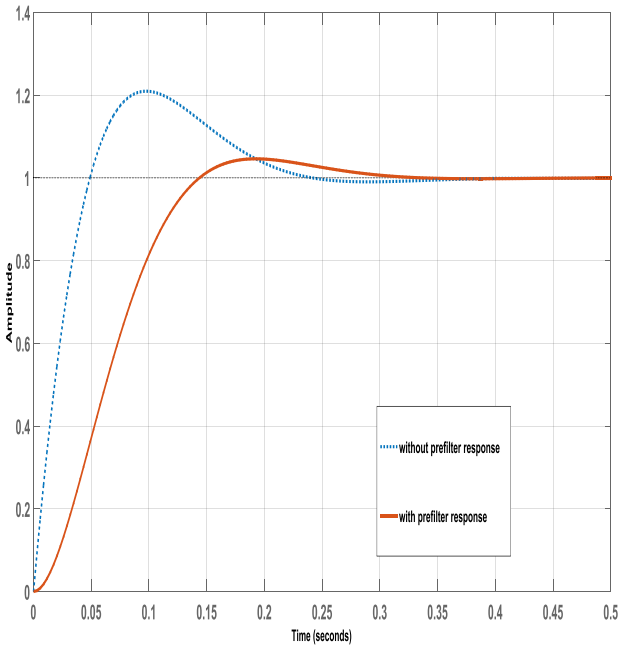

Fig.(4): step response of PI-controller

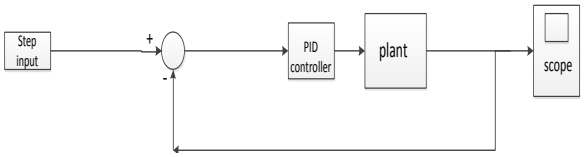

Fig.(5): Block diagram of the system controlled using PI controller tuned genetically.

Table (2): GA parameters.

GA property	Value / Method
Population size: Max. number of generations:	58 200
Performance index/ fitness function	Mean square error
Selection method	Stochastic uniform
Crossover method	Constraint dependent
Crossover fraction	0.8
Mutation method	Constraint dependent

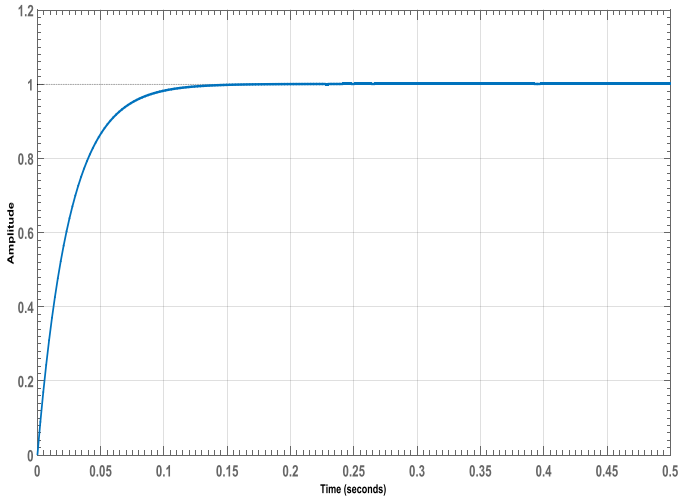

Fig.(6): Step response of the system by using values of GA controller parameters.

C. *Design of Linear Quadratic Regulator (LQR) Controller*

The theory of optimal control is concerned with operating a dynamic system at minimum cost. The Linear Quadratic Regulator (LQR) provides an optimal control law for a linear system with a quadratic performance index by calculating the gain matrix K such that it balances between the acceptable response and the amount of control energy required by minimizing the performance index [8]. This is given in equation (8).

$$J = \int_0^{\alpha} (\mathrm{x}^T \mathrm{Q}\mathrm{x} + u^T R u)dt \qquad (8)$$

where:

J cost function

X state vector

U control vector

Q weights for the state vector

R weights for the control vector

By assuming that matrices Q and R are diagonal, the cost function J is reduced to the form given in equation (9):

$$J = q_1 x_1^2 + \ldots + q_n x_n^2 + r_1 u_1^2 + \ldots + r_m u_m^2 \qquad (9)$$

It is required to find the gain matrix K that minimize the cost function J. Minimization of J causes to move x to zero with as little control energy and state deviations as possible.

Simulation of the system stabilization loop that controlled by LQR controller is carried out and the tuning of LQR controller was determined by changing the nonzero elements in the *Q* matrix where Q_{11} is used to weight the outer gimbal angular velocity and Q_{22} is used to weight the inner gimbal angular velocity. The input weighing matrix *R* will remain at 1. Equation (10), and equation (11) show the values of *Q* and *R*.

.

$$Q = \begin{bmatrix} 700 & 0 \\ 0 & 110 \end{bmatrix} \qquad (10)$$

$$R = \begin{bmatrix} 1 & 0 \\ 0 & 1 \end{bmatrix} \qquad (11)$$

The resulting feedback gain matrix K is:

$$K = \begin{bmatrix} 26.359 & 0.0189 \\ 0.0476 & 10.3905 \end{bmatrix} \qquad (12)$$

Figure (7) shows the system response to a unit step input. The system requirements discussed are satisfied. The controlled system has settling time T_S=0.236s, percentage overshoot P.O=0%, and zero steady state error.

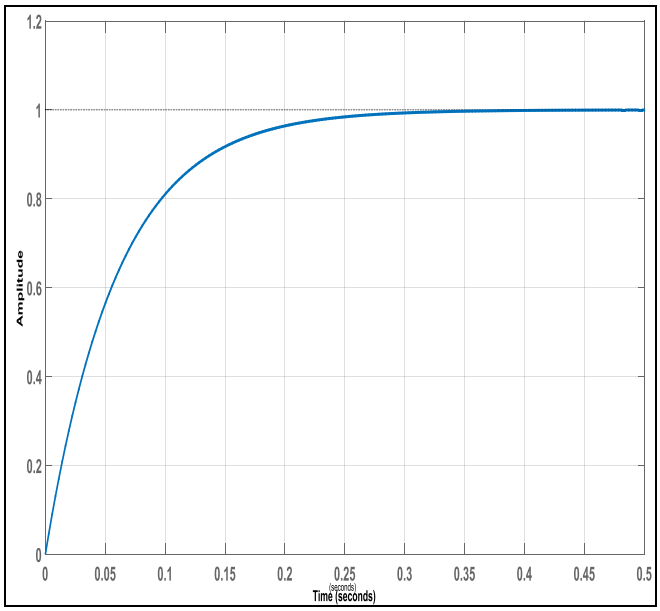

Fig.(7): Closed loop response with LQR controller

D. *Design of equivalent Linear Quadratic Gaussian (LQG) Controller*

Linear Quadratic Gaussian (LQG) control system is a system that contains a Linear Quadratic Regulator/Tracking controller together with a Kalman filter state estimator as shown in figure (8).

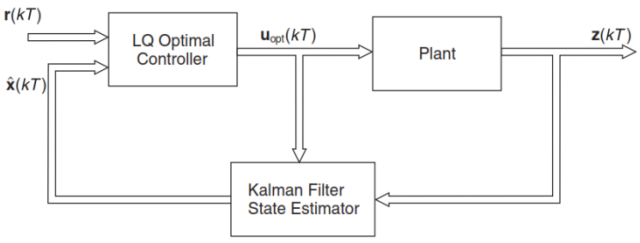

Fig.(8): Linear Quadratic Gaussian (LQG) control system [11].

In full state observer, it is assumed that all the states are available for feedback and all measurements are noise free, but the observed state vector may be subjected to noise. The best estimation of a signal is obtained by combining two noisy continuous measurements of the same signal, this method was solved by Weiner 1949 [11]. The Kalman

filter estimation is based on optimum minimum variance which is a complementary form of Kalman filter.

The goal is to control the system so that the output y(t) follows, as close as possible, the commanded output z(t).

To use LQG with reference input, the state-feedback controller is obtained in the form given in equation (13):

$$u(x) = -R^{-1}(x)B'(x)[P(x)X(t) - g(x)] \qquad (13)$$

where:

Q(x) is a symmetric positive semi-definite matrix, and R(x) is a symmetric positive definite matrix,

P(x) is a positive-definite solution of the continuous-time algebraic Riccati Equation (RE) given in (14).

$$\begin{aligned} &P(x)A(x) + A'(x)P(x) \\ &- P(x)B(x)R^{-1}(x)B'(x)P(x) \\ &+ C'(x)Q(x)C(x) = 0 \end{aligned} \qquad (14)$$

g(x) is a solution of the continuous-time state dependent non-homogeneous equation given in (15).

$$\begin{aligned} g(x) = -([A(x) - B(x)R^{-1}(x)B'(x)P(x)]')^{-1} \\ * C'(x)Q(x)z(x) \end{aligned} \qquad (15)$$

The resulting algebraic RE-derived trajectory is the solution of the closed-loop dynamics as in (16).

$$\begin{aligned} \dot{x}(t) = [A(x) - B(x)R^{-1}(x)B'(x)P(x)]x(t) \\ + B(x)R^{-1}(x)B'(x)g(x) \end{aligned} \qquad (16)$$

Simulation of the system stabilization loop that controlled by LQG controller is carried out on the system. Fig.(**9**) shows the output response of the system by using a Kalman filter compared to the step response of the system in case of using LQR controller. As it can be seen the LQG achieve an almost identical response to LQR with settling time T_S=0.0236, percentage overshoot P.O=0% and zero steady state error, in presence of noise and states estimation.

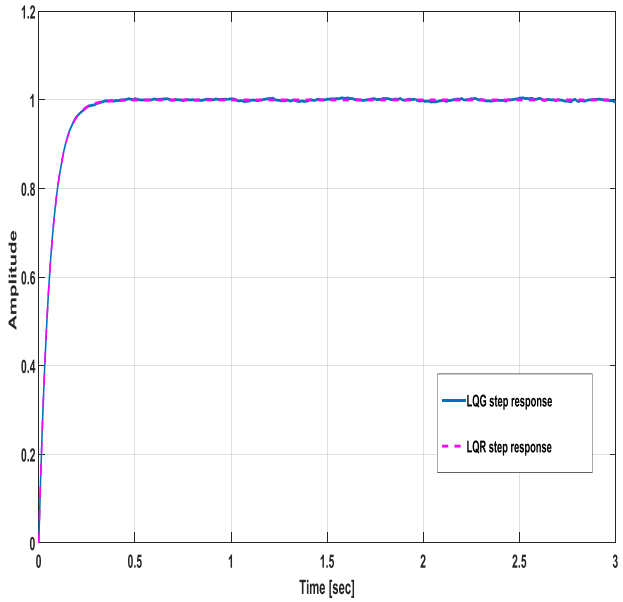

Fig.(9): Step response of the system controlled using LQG compared to the step response of the system controlled using LQR (approximately identical).

E. H_∞ Controller

The methods of H_∞ synthesis are especially powerful tools for designing robust multivariable feedback control systems to achieve singular value loop shaping specifications. The standard H_∞ control problem is sometimes also called the H_∞ small gain problem. The small gain theorem states that if a feedback loop consists of stable systems, and the product of all their gains is smaller than one, then the feedback loop is stable.

Assume that all inputs of the loop are represented by V(s), the input V(s) is founded by passing a mathematically bounded normalized input $V^1(s)$ through a transfer function block W(s), called the input weight as shown in figure (10).

Equation (17) shows this mathematical representation.

$$V(s) = W(s)\,V^1(s) \qquad (17)$$

Fig.(10): Transformation of a normalized bounded input.

Weighting functions, which reflect the frequency and time domain requirements, must be selected. A good feedback design for a particular system is obtained by selection of the frequency dependent weighting functions. At low frequency the system is required to be insensitive to disturbances while at high frequency it is required to filter out unwanted noise signals. The selection of error and output weighting functions does not involve precise rules but general guidelines gained from experience practice can be outlined. It is difficult to give rules for ensuring certain behavior because it is a matter of trade off for satisfying a number of conflicting criteria at the same time [11].

The H_∞ design problem can be formulated as follows; The generalized plant P, which is defined from the inputs $[u_1 u_2]^T$ to the outputs $[y_1 y_2]^T$, can be expressed in terms of its state space realization as in (18):

$$P(s) = \begin{bmatrix} A & B_1 & B_2 \\ C_1 & D_{11} & D_{12} \\ C_2 & D_{21} & D_{22} \end{bmatrix} \qquad (18)$$

It is required to find a stabilizing feedback control law u_2 such that the norm of the closed-loop transfer function matrix $T_{y_1 u_1}$ is small [15][16].

where:

$$u_2(s) = C(s)\,y_2(s) \qquad (19)$$

$$T_{y_1 u_1} = P_{11}(s) + P_{12}(s)[I - C(s)P_{22}(s)]^{-1}C(s)P_{21}(s) \qquad (20)$$

The state-space model of an augmented plant P(s) with weighting functions $W_p(s)$, $W_u(s)$, and $W_t(s)$ which penalize the error signal, control signal, and output signal, respectively, is shown in figure (11). The closed-loop transfer function matrix is the weighted mixed sensitivity.

where,

S the sensitivity function.
T the complementary sensitivity function (T=1-S).
L denotes the loop transfer function (L=PC).

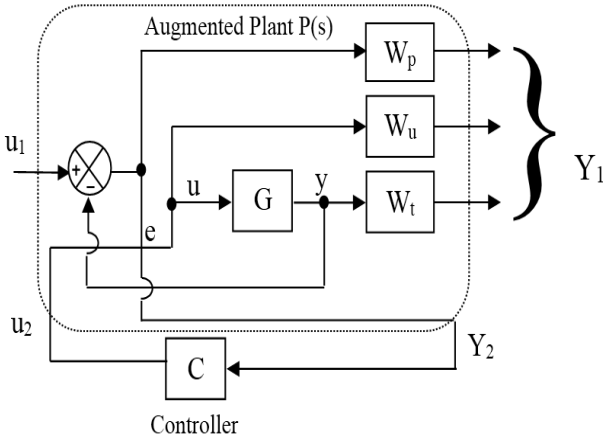

Fig.(11): Augmented Plant P(s).

Simulation of the system stabilization loop that controlled by H_∞ controller is carried out. Figure (12) shows the system step response by using H_∞ controller. The figure shows a satisfactory response with Settling time T_S=0.0702, percentage overshoot P.O=8.46% and zero steady state error.

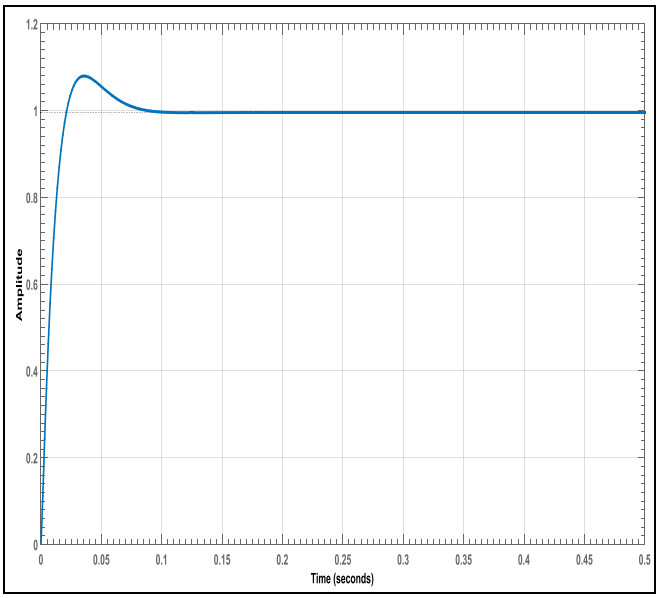

Fig.(12): The system step response by using H_∞ controller.

IV. Response Comparative Analysis

In this section, all the designed controllers for the stabilization loop are compared. Figure (13) shows the step responses of the stabilization loop with different designed controllers. It can be seen that there are many differences between the responses characteristics.

Table (3) summarizes all the step response parameters of the controlled system. It can be seen from figure (13) and table (3) that H_∞ and genetically tuned PI (GA-PI) controllers achieve the best output response. The H_∞ controller has the fastest settling time of 0.07 s, while the PI controller has the slowest settling time of 0.241 seconds. For the percentage overshoot, H_∞ controller has the highest overshoot among all controllers. Finally, all controllers achieve a zero steady state error.

Table (3): Comparison of output response parameters of all proposed controllers.

	PI	GA-PI	LQR	LQG	H_∞
Percentage overshoot	4.6%	0.077%	0%	0%	8.4%
Settling time	0.241s	0.0966s	0.236s	0.236s	0.07s
Steady state error	0	0	0	0	0

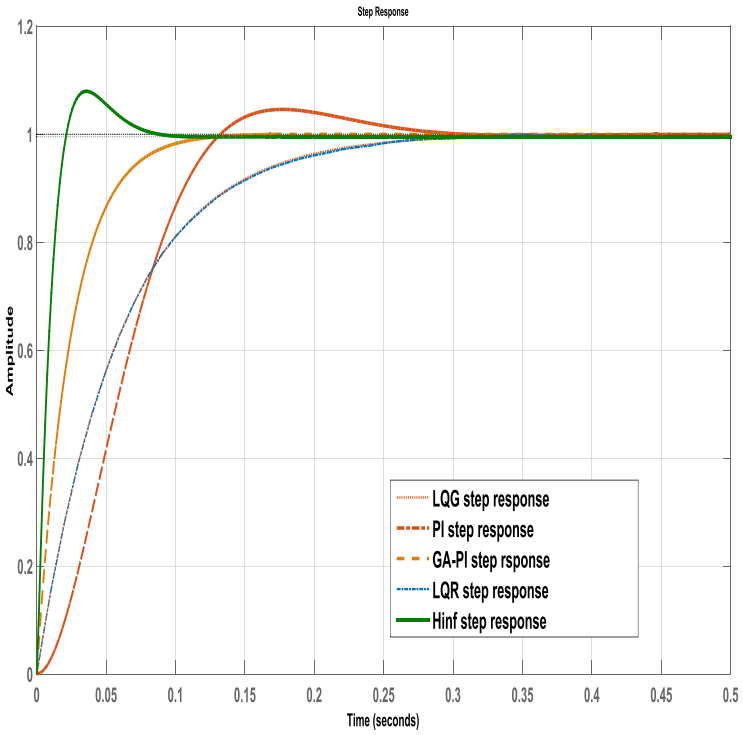

Fig.(13): Comparison between step responses of all proposed control techniques

V. Robustness Analysis

To compare performances of the designed controllers from robustness point of view, the system will be subjected to some degree of model uncertainty by changing the values of payload parameter.

A. *Robustness of PI controller*

Figure (14) shows the step response of the controlled system when the payload is changed up to 50% of its value.

The controlled system performance is accepted up to 9% of the payload original value. For 10% uncertainty, the controlled system performance is unacceptable. The settling time exceeds the required limit which is 0.25s. The output response parameters of the PI controller for 10% uncertainty are: settling time = 0.254s, percentage overshoot= 5.98%, and zero steady state error.

By increasing the degree of payload uncertainty up to 50% the system response is totally unacceptable as it can be seen from the figure. The settling time in this case is 0.29s.

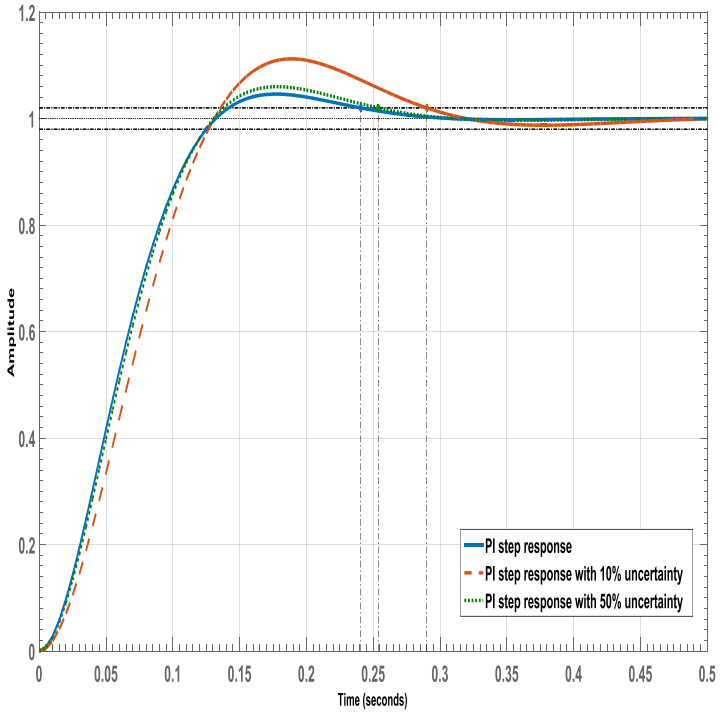

Fig.(14): Step response of PI controlled system by changing payload uncertainty up to 50%.

B. *Robustness of GA-PI*

Figure (15) shows the step response of the controlled system when the payload is changed up to 70% of its original value.

The GA-PI controlled system performance is acceptable up to 63% of the payload original value. The GA-PI controlled system response for 63% uncertainty is shown in figure (15). It can be seen from this figure that the settling time is 0.25s, the percentage overshoot is 0%, and a zero steady state error is achieved.

By increasing the degree of model uncertainty up to 70% the system response is totally unacceptable. It can be seen from figure (15) that the settling time is 0.32s.

C. *Robustness of LQR*

Figure (16) shows the step response of the system controlled using LQR when the payload is changed up to 20% of its original value.

The LQR controlled system performance is acceptable up to 9% of the payload original value. The LQR controlled system response for 10% uncertainty is unacceptable as shown in figure (16). It can be seen from this figure that the settling time is 0.259s, the percentage overshoot is 0%, and a zero steady state error is achieved.

By increasing the degree of model uncertainty up to 20%, the system response is totally unacceptable. It can be seen from figure (16) that the settling time is 0.283s.

D. *Robustness of LQG*

Figure (17) shows the step response of the system controlled using LQG when the payload is changed up to 50% of its original value.

The LQG controlled system performance is acceptable up to 9% of the payload original value. The LQR controlled system response for 10% uncertainty is unacceptable as shown in figure (17). It can be seen from this figure that the settling time is 0.259s, the percentage overshoot is 0%, and a zero steady state error is achieved.

By increasing the degree of model uncertainty up to 50%, the system response is totally unacceptable. It can be seen from figure (17) that the settling time is 0.36s.

It can be also noticed that the robustness of the LQR and the LQG are similar because the design of the LQG controller is based on the design of LQR controller in this case.

E. *Robutness of H_∞*

Figure (18) shows the step response of the system controlled using H_∞ controller when the payload is changed up to 90% of its original value.

It can be seen from figure (18) that the H_∞ controller keeps acceptable system performance when the payload is changed up to 90% of its original value.

The step response of the system controlled using H_∞ controller when the pay load is changed up to 50% is shown in figure (18). It can be seen that the settling time obtained is 0.082s, the percentage overshoot is 9%, and the steady state error is zero.

The step response of the system controlled using H_∞ controller when the pay load is changed up to 90% is also shown in figure (18). It can be seen that the settling time obtained is 0.096s, the percentage overshoot is 9.2%, and the steady state error is zero.

It can be noticed that the best controller from robust performance point of view is the H_∞ controller followed by the GA-PI controller.

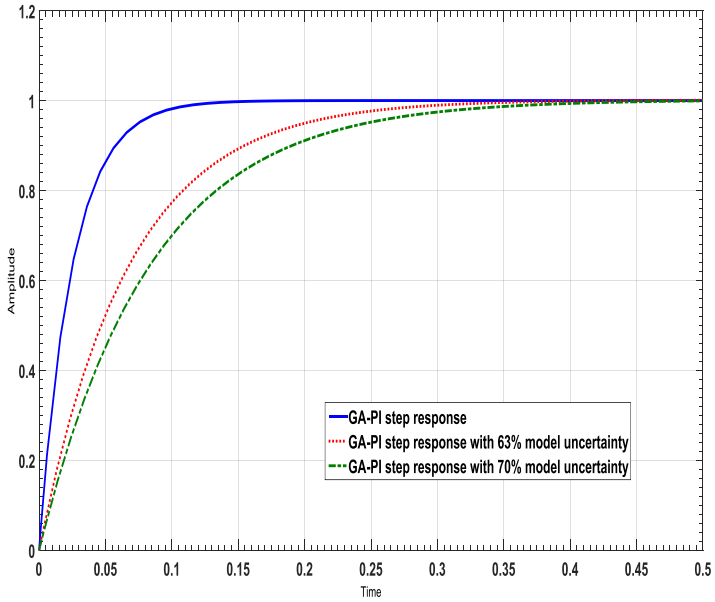

Fig.(15): Step response of the system controlled by GA-PI when the payload is changed up to 70%

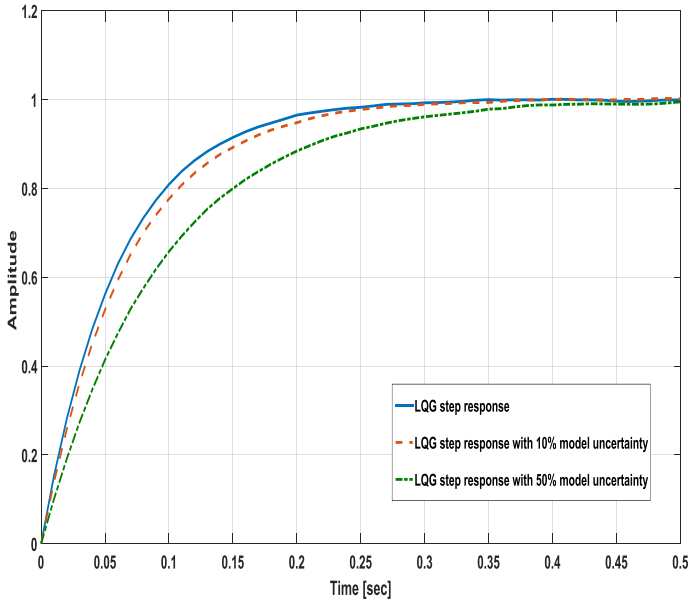

Fig.(17): Step response of the system controlled by LQG controller when the payload is changed up to 50%

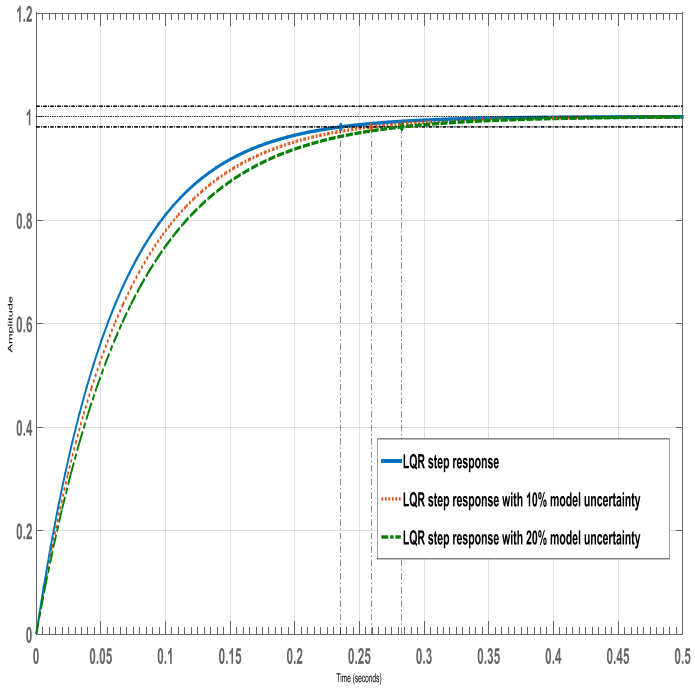

Fig.(16): Step response of the system controlled by LQR controller when the payload is changed up to 20%.

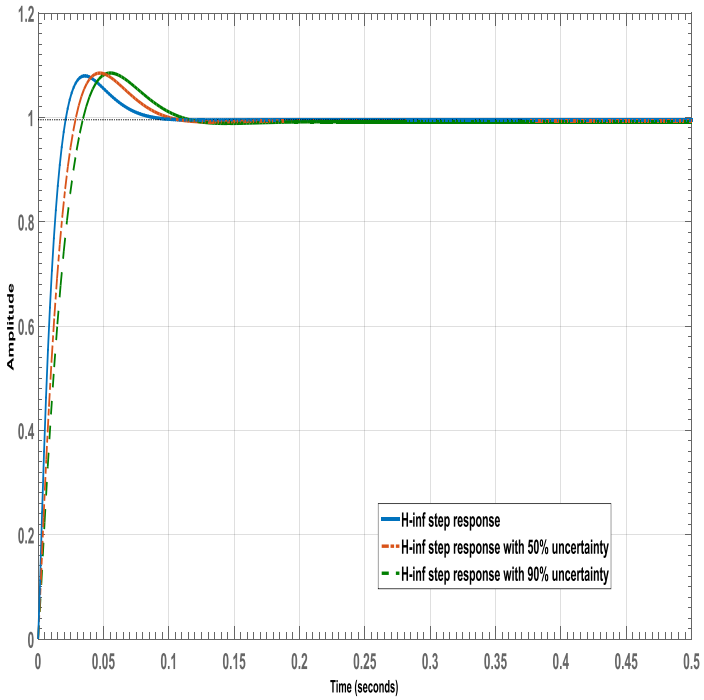

Fig.(18): Step response of the system controlled by H_∞ controller when the payload is changed up to 90%.

VI. CONCOLOSION

Different controllers are designed for LOS subsystem used in fire control system. PI controller is designed and its parameters are tuned classically and are tuned again using GA. LQR, LQG, and H_∞ controllers are also designed for the LOS stabilization subsystem.

The controlled system performances are compared in normal operating conditions and when the system is subjected to model uncertainty. It was found that all the designed controllers satisfy the system requirements in normal operating conditions. The fastest response was for H_∞ controller followed by GA-PI. Considering the percentage overshoot, it was found that the GA-PI is better than H_∞ controller. But both are acceptable.

The designed controllers are compared when the system is subjected to model uncertainty. Robust stability and robust performance are considered. From robust stability point of view, the simulation results show that the controlled system is stable for all controllers when the system is subjected to model uncertainty. This is because the system is a low order system. From robust performance point of view, the simulation results show that the best performance is achieved by H_∞ controller followed by GA-PI controller.

From the results obtained based on normal operating conditions and when the system is subjected to model uncertainty, it was found that H_∞ controller and GA-PI controller are the best in the case studied.

REFERENCES

[1] A. Roshdy, Y. Z. Lin, C. Su, H. F. Mokbel, and T. Wang, "Design and performance of non-linear fuzzy logic PI controller for line of sight stabilized platform," in *Optoelectronics and Microelectronics (ICOM), 2012 International Conference on*, 2012, pp. 359-363.

[2] K. Tan, T. Lee, A. Mamun, M. Lee, and C. Khoh, "Composite control of a gyro mirror line-of-sight stabilization platform—design and auto-tuning," *ISA transactions*, vol. 40, pp. 155-171, 2001.

[3] Y. Han, Y. Lu, and H. Qiu, "An improved control scheme of gyro stabilization electro-optical platform," in *Control and Automation, 2007. ICCA 2007. IEEE International Conference on*, 2007, pp. 346-351.

[4] T. Zhiyong, P. Zhongcai, and W. Baolin, "Research on Image-Stabilizing System Based on Gyro-Stabilized Platform with Reflector," in *Proceeding of SPIE*, 2008, pp. 71281A1-71281A6.

[5] J. Hilkert and S. Cohen, "Development of mirror stabilization line-of-sight rate equations for an unconventional sensor-to-gimbal orientation," in *SPIE Defense, Security, and Sensing*, 2009, pp. 733803-733803-12.

[6] L. Said, L. Sheng, N. Farouk, and B. Latifa, "Modeling, Design and Control of a Ship Carried 3 DOF Stabilized Platform," 2012.

[7] J. Basilio and S. Matos, "Design of PI and PID controllers with transient performance specification," *Education, IEEE Transactions on*, vol. 45, pp. 364-370, 2002.

[8] R. C. Dorf and R. H. Bishop, "Modern control systems," 1998.

[9] K. Ogata, "Modern control engineering."

[10] H. F. Mokbel, L. Q. Ying, A. Roshdy, and C. G. Hua, "Modeling and optimization of Electro-Optical dual axis Inertially Stabilized Platform," in *Optoelectronics and Microelectronics (ICOM), 2012 International Conference on*, 2012, pp. 372-377.

[11] R. Burns, *Advanced control engineering*: Butterworth-Heinemann, 2001.

[12] A. A. Roshdy, C. Su, H. F. Mokbel, and T. Wang, "Design a robust PI controller for line of sight stabilization system," 2012.

[13] N. Thomas and D. P. Poongodi, "Position control of DC motor using genetic algorithm based PID controller," in *Proceedings of the World Congress on Engineering*, 2009, pp. 1-3.

[14] K.-F. Man, K.-S. Tang, and S. Kwong, "Genetic algorithms: concepts and applications," *IEEE Transactions on Industrial Electronics*, vol. 43, pp. 519-534, 1996.

[15] G. Halikias, "An affine parametrization of all one-block H∞-optimal matrix interpolating functions," *International Journal of Control*, vol. 57, pp. 1421-1441, 1993.

[16] R. Sutton, G. Halikias, A. Plummer, and D. Wilson, "Robust control of a lightweight flexible manipulator under the influence of gravity," in *Control Applications, 1997., Proceedings of the 1997 IEEE International Conference on*, 1997, pp. 300-305.